

Copolyester Studies. II. Melting and Crystallization Behavior of Tetramethylene Terephthalate-Tetramethylene Sebacate Copolymers

W. MARRS, R. H. PETERS, and R. H. STILL, *Department of Polymer and Fibre Science, UMIST, Manchester, England*

Synopsis

The melting and crystallization behavior of poly(tetramethylene terephthalate) and its copolymers with tetramethylene sebacate (> 20 mol %) has been studied using differential scanning calorimetry (DSC). The effect of the sebacate concentration on equilibrium melting temperature and crystallization behavior is discussed in terms of the theory of equilibrium crystallization of random copolymers. The multiple-melting behavior of these systems is described and interpreted in terms of the theory of equilibrium melting of chain-folded crystals, together with molecular fractionation during crystallization and melting and recrystallization during the DSC scan.

INTRODUCTION

In a previous paper¹ we described the preparation and detailed characterization of copolymers of tetramethylene terephthalate and tetramethylene sebacate containing up to 20 mol % of the latter. We now report the melting and crystallization behavior of poly(tetramethylene terephthalate) 4GT and the copolymer systems.

In view of the detailed information available on the thermal properties of poly(ethylene terephthalate) 2GT, it is perhaps surprising that little has been published on other useful members of the poly(methylene terephthalate) series. Thus for 4GT, which has begun to challenge 2GT in some of its applications, only the melting temperature²⁻⁴ and some aspects of its crystallization behavior^{5,6} have been reported. In general, there is a paucity of relevant detailed information on these materials.

EXPERIMENTAL

Materials

4GT and the copolymers were prepared and characterized as previously described.¹ 2GT was supplied by ICI Ltd. as a cast amorphous film and poly(hexamethylene terephthalate), 6GT, was prepared by a conventional melt condensation process.¹

Apparatus and Procedure

Thermal measurements were made using a Perkin-Elmer differential scanning calorimeter (DSC) model 2. Samples in the form of thin disks were cut from compression-molded polymer films.¹ The sample (≈ 5 mg) was encapsulated

in an aluminum pan, and an empty pan of the same weight acted as the inert reference material. Argon was used as the purge gas at a flow rate of 20 ml/min.

Equilibrium Melting Temperatures

The equilibrium melting temperatures of the polymers were determined by an extrapolation method due to Hoffman and Weeks.⁷ The procedure used was as follows. A sample was held in the instrument at a temperature of 25°C above the observed DSC2 melting temperature¹ for 20 min. The sample was then cooled at 320°C/min to a preset crystallization temperature and allowed to remain at this temperature for 60 min. The sample and reference were then cooled at 320°C/min to 47°C (ambient for the instrument) and finally scanned through the melting region at 20°C/min. For each crystallization temperature a new sample of polymer was used. Results were obtained at 2.5°C intervals using a crystallization temperature range of 50°C.

In order to assess the effect of cooling the sample to 47°C after the crystallization period, a series of control experiments were performed in which this cooling step was omitted. After crystallization, the sample was scanned from the crystallization temperature at 20°C/min through the melting region. A second series of control experiments was also carried out to determine the effect of crystallization time in the range 5–60 min.

Isothermal Crystallization Rates

The isothermal crystallization rates of the polymers were obtained from DSC2 measurements using the method due to Knox.⁸ A polymer sample was held in the instrument for 20 min at a temperature 5°C above its predetermined equilibrium melting temperature. The sample was then cooled at 320°C/min to the desired, preset crystallization temperature and a time-based record of the isothermal crystallization process obtained. Data were obtained at temperatures where the degree of supercooling ΔT was 37.5, 40, 42.5, 45, and 50°C, ΔT being defined as the equilibrium melting temperature T_{m^*} minus the crystallization temperature T_c .

RESULTS AND DISCUSSION

Equilibrium Melting Temperatures

From their theory of equilibrium melting of a high-molecular-weight homopolymer, Hoffman and Weeks⁷ have derived the relationship

$$T_{m,obs} = T_{m^*} (1 - 2\sigma_e/\Delta H_f l) \quad (1)$$

where σ_e is the end-surface free energy of the crystal, l is the step height or lamellar thickness, and ΔH_f is the heat of fusion per unit volume of the crystal. The authors postulate that for crystals grown in the chain-folded pattern, one dimension of the crystal, i.e., the step height, will retain a value close to that of the primary or growth nucleus, whereas the a and b dimensions continue to grow to large size. The lamellar thickness l will vary with the crystallization temperature T_c as $1/\Delta T$ because of the nature of the nucleation-controlled growth

mechanism in chain-folded crystals. Equation (2) describes a straight line for a plot of $T_{m,obs}$ against T_c , where the equilibrium melting temperature is defined as the intersection of this line with $T_{m,obs} = T_c$.

$$T_{m,obs} = T_{m*} (1 - 1/2\beta) + T_c/2\beta \quad (2)$$

where β is a constant relating the mean step height of the crystals to the mean step height of the primary or growth nuclei.

The theory of Hoffman and Weeks applies strictly to homopolymers. However, Flory⁹ and Baker and Mandelkern¹⁰ have suggested very similar theories for random copolymers that provide results in accord with those for homopolymers.

During the determination of equilibrium melting temperatures of the polymers up to four melting endotherms were observed on the DSC traces. One such trace is shown in Figure 1, where the endotherms are labelled I-IV. Only one of these endotherms, II, exhibited the behavior expected from the various theories of equilibrium melting,^{7,9,10} and it was this peak that was taken to be $T_{m,obs}$. The determination of the equilibrium melting temperature of one of the copolymers is shown in Figure 2. The effect of the crystallization temperature on the peak temperature of all four endotherms is shown in Figure 2 and discussed in detail later in the section on multiple melting.

An important, practical consideration in the determination of equilibrium melting temperatures by extrapolation methods was shown by Hoffman and Weeks to be the effect of residence time at T_c . The theoretical considerations are based on the assumption that the step height of the crystal l remains at a certain value, dependent on T_c , until the crystal has melted. Long residence times at T_c may involve an increase in l through complex chain rearrangements, thereby reducing the extrapolated value of T_{m*} . Control experiments indicated, however, that the value of $T_{m,obs}$ obtained using residence times of 60 min showed no significant difference relative to a residence time of 5 min.

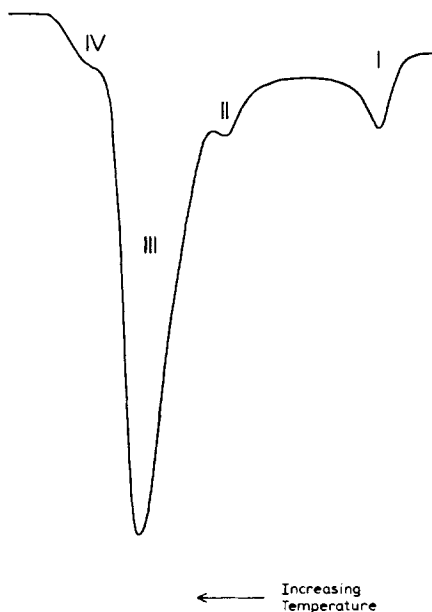


Fig. 1. Typical multiple-melting endotherms.

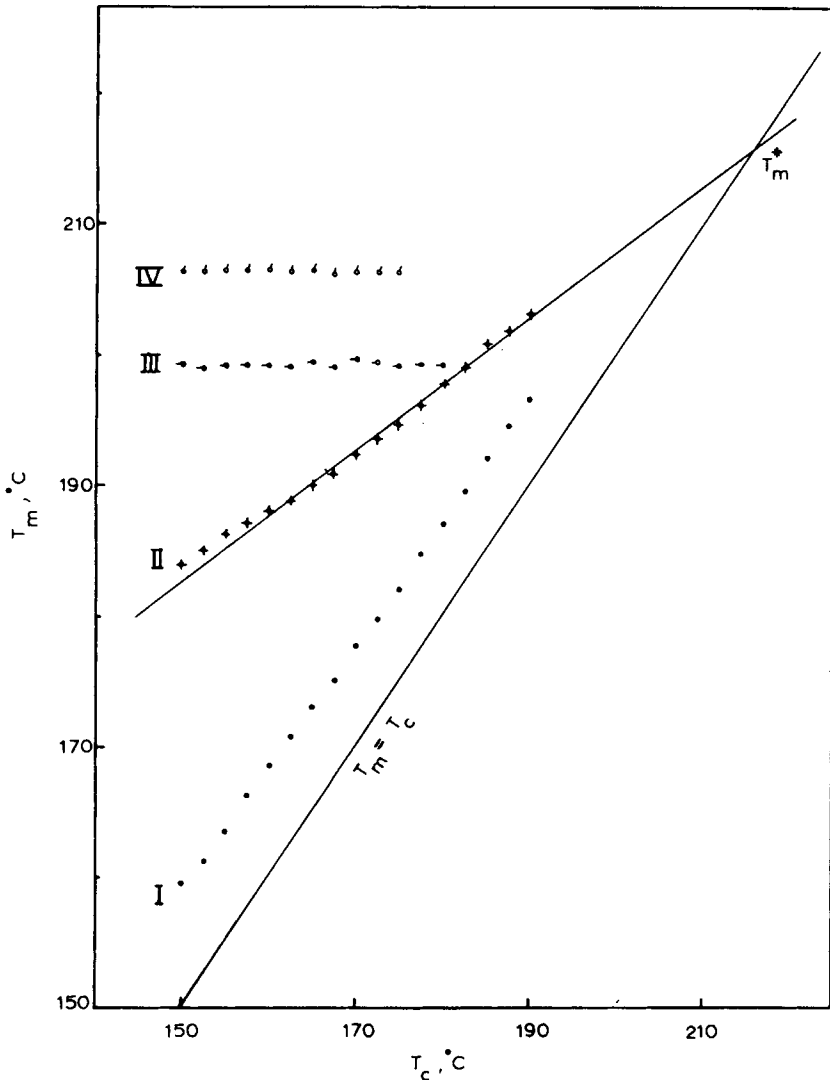


Fig. 2. Determination of equilibrium melting temperature.

Values obtained for the equilibrium melting temperature of the polymers (Table I) are, as expected, significantly higher than the normally determined DSC2 or hot-stage polarizing microscope values.¹ The value of 236°C obtained for 4GT is also higher than previously reported data obtained by other methods.²⁻⁶ The slope of the line $T_{m,obs}$ against T_c is, as shown in Table I, approximately 0.5 for each system and is in accord with the data for other copolymer systems.¹¹

A slope of 0.5 corresponds to a value of 1 for β in eq. (2) and leads to the general relationship

$$T_{m,obs} = (T_{m*} + T_c)/2 \quad (3)$$

Such a value of β suggests, from the theory of Hoffman and Weeks, that the step height distribution of the grown lamellae is similar to that of the primary or growth nuclei and is therefore in agreement with theoretical considerations. A

TABLE I
 Equilibrium Melting Data

| Composition, mol % sebacate | T_{m^*} , °C | Slope of line, $T_{m,obs}$ vs T_c |
|--------------------------------|----------------|--|
| 0 | 236 | 0.55 |
| 5 | 230.5 | 0.58 |
| 10 | 222 | 0.50 |
| 15 | 215.5 | 0.50 |
| 20 | 208 | 0.47 |

β value of 1 also justifies the residence time of 60 min at T_c , since a larger value would be expected for unduly long residence times because of lamellar thickening caused by chain-mobility effects.⁷

The decrease in T_{m^*} with increasing sebacate content is in agreement with the theory of equilibrium melting of random copolymers.⁹ This theory predicts a depression in melting temperature caused by the noncrystallizing units according to the equation

$$\frac{1}{T_m} - \frac{1}{T_m^0} = -\frac{R}{\Delta H_f} \ln X \quad (4)$$

where T_m is the melting temperature of the copolymer, T_m^0 is the melting temperature of the homopolymer, ΔH_f is the heat of fusion per repeat unit of the homopolymer, and X is the mole fraction of crystallizable units. The melting point depression is dependent on the heat of fusion per mole of the crystallizing unit and on the sequence propagation probability p , which it is suggested in random copolymers can be identified with X .⁹ The melting temperature data given in Table I have been plotted in Figure 3 according to the above equation. From the slope of the line in Figure 3, a value of 3870 cal mol⁻¹ is obtained for the heat of fusion of 4GT, which is significantly lower than the value of 7600 cal mol⁻¹ obtained by Conix and Van Kerpel⁴ from the polymer-diluent method and 7500 cal mol⁻¹ calculated theoretically by Kirshenbaum.¹²

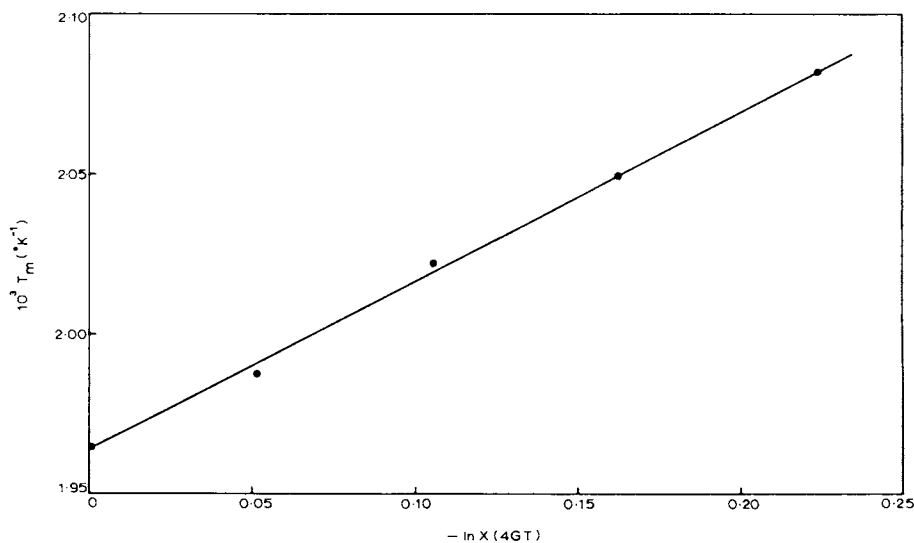


Fig. 3. Determination of heat of fusion of 4GT.

The random-copolymer equation (4) has been reported to give values that are lower than expected,¹³⁻¹⁶ and this has been attributed by Mandelkern¹⁷ to the experimental difficulty in determining the temperature at which the last crystallite has melted. Mandelkern has shown that this situation will lead to a low heat of fusion even though the relationship between $1/T_m$ and $\ln X$ remains linear. In the present case, however, it would seem inappropriate to invoke this explanation, since the T_m values substituted into eq. (4) in this study were the equilibrium melting temperatures, i.e., theoretically the temperature at which a crystal with the equilibrium degree of crystal perfection should melt. It would appear more likely, therefore, that the low heat of fusion value was caused by the noncrystallizing units rendering adjacent crystallizable units noncrystallizable because of their difference in size and character, leading to a wrong assessment of X in eq. (4). A similar explanation has been invoked by Onder et al.¹⁶ for the low heat of fusion value obtained from ethylene adipate/toluene-2,4-di-isocyanate copolymers. The latter authors have shown that a more reasonable heat of fusion value is obtained if each toluene di-isocyanate unit is considered to render six ethylene adipate units noncrystallizable.

Isothermal Crystallization Rates

The isothermal crystallization rates of the polymers have been measured in terms of the half-time of the process $t_{1/2}$, where the latter is defined as the time required to crystallize half of the available crystallizable material. Crystallization rates were determined in the region between $T_{c\max}$ and T_{m*} as a function of the degree of supercooling ΔT .

The crystallization curves were analyzed by means of the Avrami equation

$$(1 - X_t) = \exp(-Zt^n) \quad (5)$$

in the form

$$\log[-\ln(1 - X_t)] = n \log t + \log Z \quad (6)$$

where X_t is the weight fraction of crystallized material at time t , Z a rate constant, and n the Avrami exponent. The left-hand side of eq. (6) can be plotted against $\log t$ and should yield a straight line of slope n .

The data presented in Table II shows that for any particular polymer studied, the crystallization rate increases as ΔT is increased. Similarly, as sebacate content increases the rate of crystallization decreases. The crystallization rates of 4GT and the 5% copolymer at $\Delta T = 50^\circ\text{C}$ were too rapid to be measured using the DSC method.

The degree of supercooling required to produce a crystallization half-time of

TABLE II
Effect of Composition and Supercooling on Crystallization Rate

| Composition mol % sebacate | $t_{1/2}$ (sec) at a ΔT ($^\circ\text{C}$) of | | | | |
|-------------------------------|---|-----|------|----|----|
| | 37.5 | 40 | 42.5 | 45 | 50 |
| 0 | 102 | 60 | 32 | 28 | — |
| 5 | 105 | 68 | 38 | 32 | — |
| 10 | 190 | 103 | 81 | 55 | 36 |
| 15 | 235 | 143 | 96 | 60 | 43 |
| 20 | 306 | 167 | 135 | 94 | 56 |

60 sec is shown in Table III. The degree of supercooling increases with increasing sebacate content and indicates the effect of the sebacate units on the attenuation of the crystallization rate. Similarly, Figure 4, a plot of the reciprocal of $t_{1/2}$ against T_c , also describes the effect of composition on crystallization rate, showing the reduction in temperature required to produce a certain $t_{1/2}$ as the sebacate content increases. With only 5% sebacate units present, the effect on the crystallization rate is relatively small; however, as the concentration of sebacate approaches 20 mol %, a large reduction in rate is apparent. This is of course to be expected from the theory of equilibrium crystallization of random copolymers^{9,18} and is in accord with results from other copolymer systems.¹⁹⁻²¹

The heat of crystallization liberated during the isothermal process was measured for each copolymer, and the results are shown in Table IV as a function of the degree of supercooling. The data reveal that, as expected, at any particular degree of supercooling, the heat of crystallization decreases as the sebacate content increases. However, it can also be seen that for any particular polymer, the heat of crystallization, and therefore the degree of crystallinity, increases as the degree of supercooling and crystallization rate increase. This effect may be due to the fact that the process of rejection of structural irregularities is not as efficient at faster crystallization rates, and therefore more imperfect material is included within the crystallites.

Figure 5 shows a typical Avrami plot for the homopolymer 4GT, whereas values of the Avrami exponent n , calculated from the initial slope of such plots, are shown in Table V. Sharples²² has suggested that the analysis of crystallization rate data by the Avrami equation must be treated with some caution if a mechanistic evaluation of the process is to be evoked. However, it is still possible to discuss qualitatively the apparent trends. Thus the data in Table V reveals an increase in the value of n as ΔT decreases and similarly a small effect of composition on the value of n .

A similar observation of increase in the value of n with crystallization temperature has been reported by Gogolewski and Turska²¹ in the study of the crystallization kinetics of some copolyamides. The latter authors suggested that two different nucleation mechanisms may be responsible for the phenomenon.

It is interesting to compare the results of Gilbert and Hybart,⁵ who studied the crystallization rates of 4GT by both dilatometry and DSC, with the data obtained in the present work. The latter authors reported n values of 2.6 by DSC and 2.8 by dilatometry in the temperature range of $\Delta T = 21-27^\circ\text{C}$. Table V shows that for 4GT, n increases from 2.0 at $\Delta T = 45^\circ\text{C}$ to 2.5 at $\Delta T = 37.5^\circ\text{C}$. Together the results indicate a definite increase in n with increasing crystallization temperature.

TABLE III
Supercooling Required for Crystallization Half-Time of 60 sec

| Composition, mol % sebacate | T_c , $^\circ\text{C}$ | ΔT , $^\circ\text{C}$ |
|--------------------------------|--------------------------|-------------------------------|
| 0 | 196 | 40 |
| 5 | 190 | 40.5 |
| 10 | 178 | 44 |
| 15 | 170 | 45 |
| 20 | 159 | 49 |

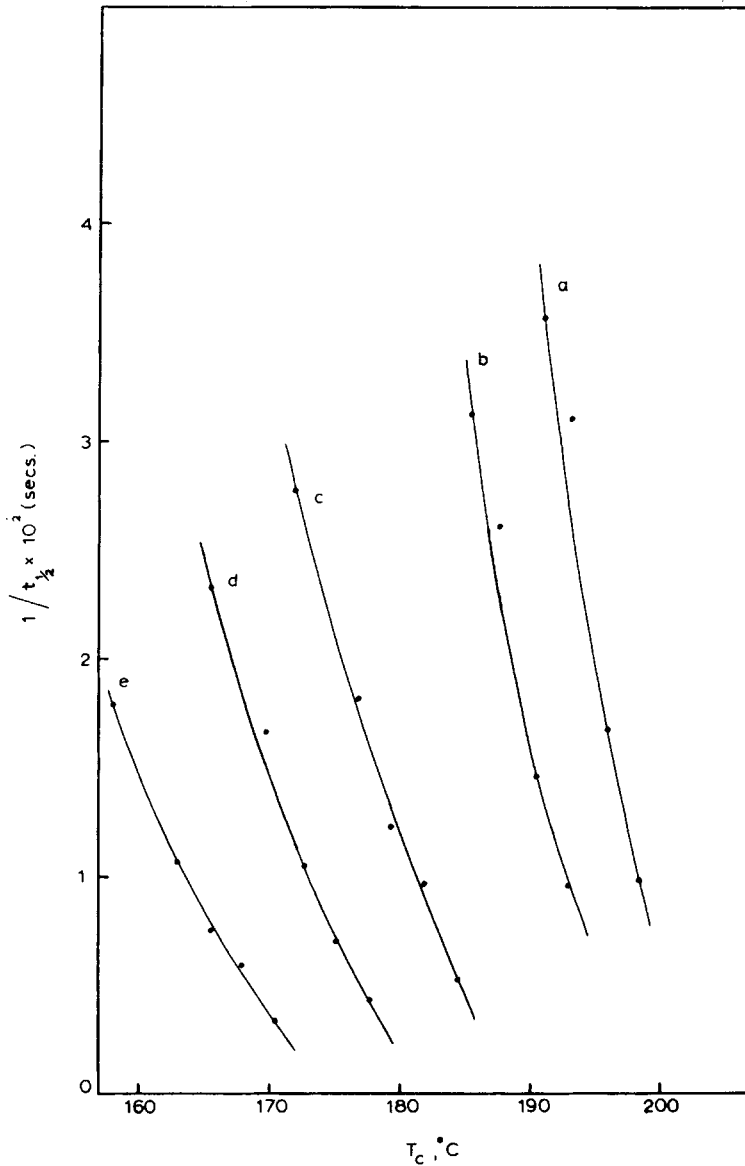


Fig. 4. Isothermal crystallization half-times: (a) 4GT, (b) 5% sebacate, (c) 10% sebacate, (d) 15% sebacate, (e) 20% sebacate.

Multiple-Melting Behavior

The behavior of the four endotherms shown in Figure 1 is dependent on both crystallization temperature and time. In this study the effects of crystallization temperature only are reported. Thus Figure 6 demonstrates the effects of crystallization temperature on the multiple-melting behavior of 4GT. The copolymer systems exhibit similar trends to those observed in 4GT, and this is shown in Table VI and Figure 7 for the 15% sebacate copolymer. The four endotherms (peaks I-IV) behave in the following manner:

(1) Peak I is present even at very low crystallization temperatures. The peak

TABLE IV
Heat of Crystallization as a Function of the Degree of Supercooling

| Composition, mol % sebacate | $\Delta H_{\text{cryst.}}$ (cal mole ⁻¹) at ΔT (°C) of | | | | |
|--------------------------------|--|-------|-------|-------|-------|
| | 37.5 | 40 | 42.5 | 45 | 50 |
| 0 | 12.84 | 12.54 | 13.30 | 13.47 | — |
| 5 | 11.36 | 11.45 | 11.78 | 12.51 | — |
| 10 | 8.77 | 9.72 | 9.82 | 10.43 | 10.67 |
| 15 | 8.57 | 8.94 | 8.90 | 9.47 | 10.03 |
| 20 | 4.61 | 6.58 | 7.68 | 8.38 | 8.57 |

TABLE V
Value of the Avrami Exponent, n

| Composition mol % sebacate | Value of n at ΔT (°C) of | | | | |
|-------------------------------|------------------------------------|-----|------|-----|-----|
| | 37.5 | 40 | 42.5 | 45 | 50 |
| 0 | 2.5 | 2.2 | 2.2 | 2.0 | — |
| 5 | 2.5 | 2.2 | 2.2 | 2.0 | — |
| 10 | 2.3 | 2.2 | 2.2 | 2.0 | 1.6 |
| 15 | 2.0 | 2.1 | 2.2 | 1.9 | 1.6 |
| 20 | 2.0 | 2.2 | 2.2 | 1.9 | 1.5 |

TABLE VI
Peak Temperatures of Multiple Endotherms for 15% Sebacate Copolymer

| Crystallization temperature, °C | Peak temperature, °C | | | |
|------------------------------------|----------------------|-------|-------|-------|
| | I | II | III | IV |
| 140 | 149.5 | — | 199 | 206.1 |
| 142.5 | 152.1 | 181.5 | 198.9 | 206 |
| 145 | 154.4 | 182.3 | 198.8 | 206 |
| 150 | 159.6 | 183.9 | 199.2 | 206.3 |
| 152.5 | 161.2 | 185 | 198.9 | 206.3 |
| 155 | 163.8 | 186.3 | 199.2 | 206.4 |
| 157.5 | 166.2 | 187.1 | 199.2 | 206.4 |
| 160 | 168.6 | 188 | 199.2 | 206.5 |
| 162.5 | 170.7 | 188.8 | 199.1 | 206.4 |
| 165 | 173 | 190 | 199.4 | 206.4 |
| 167.5 | 175 | 190.6 | 199 | 206.1 |
| 170 | 177.7 | 192.3 | 199.7 | 206.3 |
| 172.5 | 179.7 | 193.4 | 199.5 | 206.2 |
| 175 | 182 | 194.4 | 199.1 | 206.2 |
| 177.5 | 184.6 | 195.9 | 199.2 | — |
| 180 | 187 | 197.7 | 199.2 | — |
| 182.5 | 189.5 | 199 | — | — |
| 185 | 192 | 201 | — | — |
| 187.5 | 194.5 | 201.8 | — | — |
| 190 | 196.4 | 203.1 | — | — |
| 192.5 | — | — | 198 | 205 |
| 195 | — | — | 198.8 | 206 |

temperature is 5–10°C above the crystallization temperature T_c and increases as T_c is increased. The peak height remains relatively small and constant in size. Peak I disappears at high crystallization temperatures.

(2) Peak II only occurs above a definite crystallization temperature. The peak height and temperature increase with increasing T_c until at some definite value of T_c it becomes the largest peak present. With further increase in crystallization

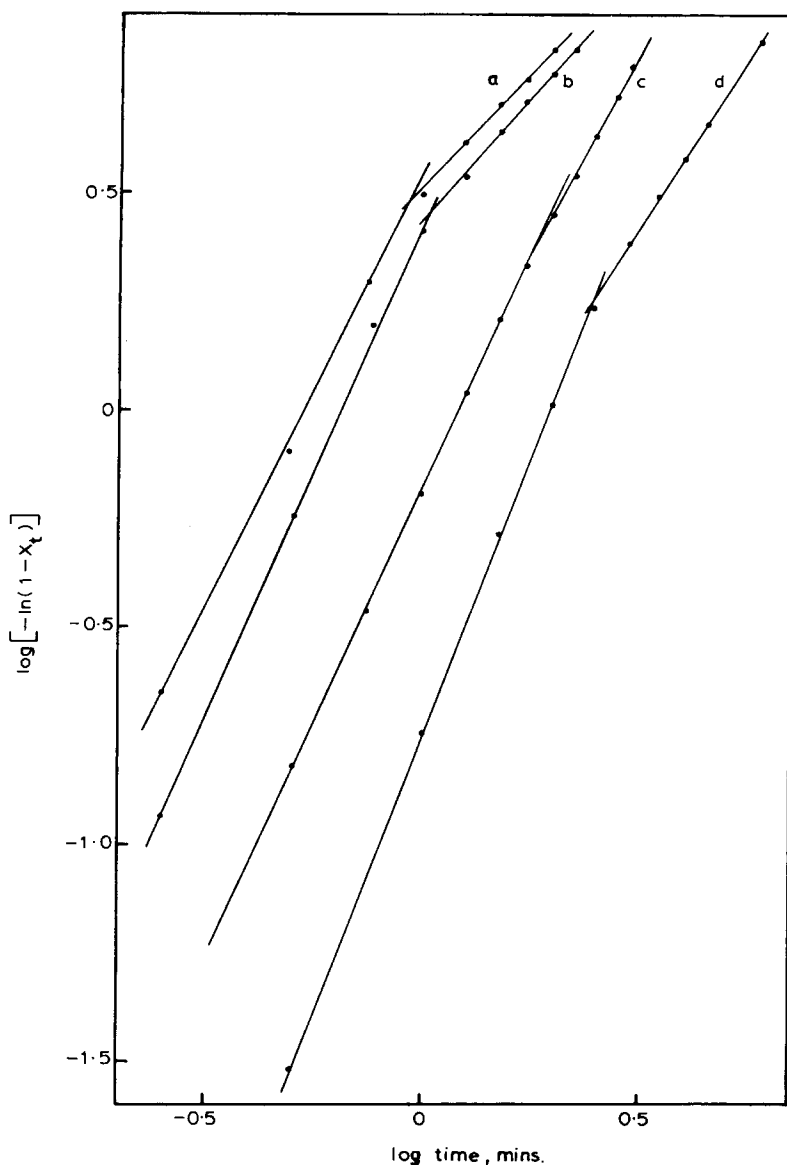


Fig. 5. Avrami analysis for 4GT at different degrees of supercooling ($^{\circ}\text{C}$): (a) $\Delta T = 45$, (b) 42.5, (c) 40, (d) 37.5.

temperature, peak II begins to diminish in size, but the peak temperature continues to increase, and ultimately the peak disappears.

(3) Peak II occurs at the same temperature irrespective of the crystallization temperature. The peak height is large at low crystallization temperatures, but at intermediate values of T_c , where peak II initially appears and begins to increase in size, the height of peak III decreases. It appears that this reduction in size of peak III is roughly equivalent to the increase in size of peak II, and at some value of T_c when peak II becomes large, peak III disappears.

(4) Peak IV also occurs at the same peak temperature irrespective of T_c and is essentially a small shoulder on the high-temperature side of peak III. This

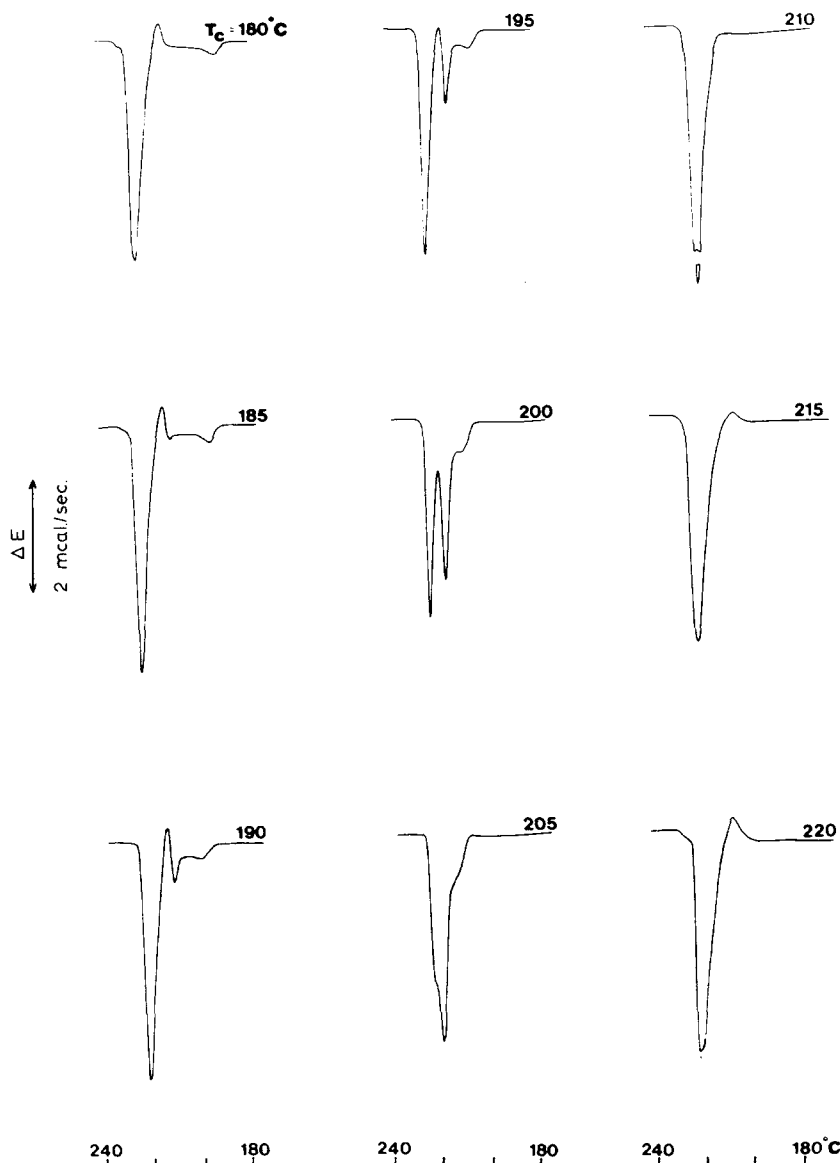


Fig. 6. Multiple-melting behavior of 4GT.

peak decreases in size and finally disappears when peak II becomes dominant. At high crystallization temperatures, however, peak IV reappears.

In addition to the four endotherms described, an exotherm is also apparent on the 4GT traces immediately prior to peak III. This exotherm is not apparent on the majority of copolymer traces because of the width and height of their endothermic peaks.

The observation of multiple-melting endotherms on DSC traces is not unusual, and in recent years the phenomenon has been reported for many crystallizable polymers, including poly(ethylene terephthalate),²³⁻²⁸ nylon 66,^{29,30} polyethylene,^{31,32} isotactic polystyrene,^{30,33} and polyoxymethylene.³⁴ In the majority of cases cited, only two endotherms have been reported, the exceptions being

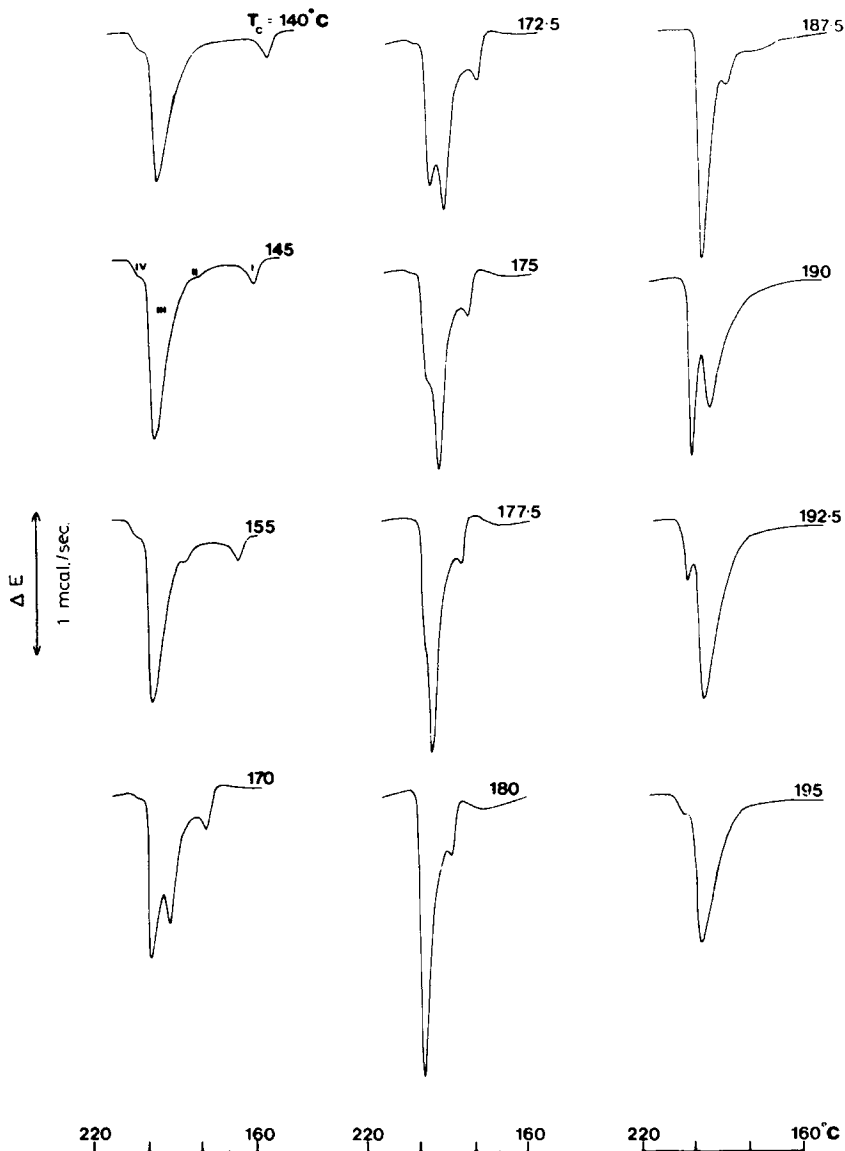


Fig. 7. Multiple-melting behavior of 15 mol % sebacate copolymer.

polyethylene and the three endotherms observed by Ikeda²⁶ for poly(ethylene terephthalate). In the present study, three endotherms were also observed for 2GT and for poly(hexamethylene terephthalate) 6GT under the conditions of test. A recent study by Hobbs and Pratt,³⁵ however, has reported two endotherms for 4GT for samples that had been cooled from the melt at rates of 5–40°C/min and then reheated in a Perkin-Elmer DSC2 machine at 5–80°C/min.

The behavior of peaks II and III is similar to the behavior of the two endotherms observed by Roberts²³ and Holdsworth and Turner-Jones.²⁴ Both the latter authors, together with Sweet and Bell²⁵ and Ikeda²⁶ have shown that the high-temperature endotherm in 2GT, which is analogous to peak III in the

present work, is due to the partial melting and recrystallization of initially small and imperfect crystals during heating in the DSC instrument. The possibility of recrystallization was initially proposed by Jaffe and Wunderlich³⁴ and subsequently extended by Ikeda,²⁶ who suggested that the absence of a crystallization exotherm was due to simultaneous melting and recrystallization. Further evidence for this can be found in our previous paper,¹ where it was shown that an increase in crystallinity occurred for both an initially amorphous and a moderately crystalline sample of 4GT during the programmed heating cycle of the DSC experiment. It is also possible that the small and imperfect crystals responsible for peak III were formed during cooling of the sample after crystallization. However, control experiments, where the cooling stage was omitted, revealed that this was not the case.

Figure 2 shows that the peak temperatures associated with peak II can be used to obtain a value for the equilibrium melting temperature using the method of Hoffman and Weeks.⁷ The theory behind such a method is applicable to high-molecular-weight polymers having crystals grown in a chain-folded pattern. The theory predicts an increase in lamellar thickness and hence melting temperature with increasing crystallization temperature, which would result in an increase in the size and sharpness of the observed DSC endotherm up to a certain limiting crystallization temperature. Above this limiting T_c , which is approximately 20°C below the equilibrium melting temperature, a rapid decrease in peak size would occur, since the crystallization rate becomes exponentially slower as T_c approaches T_{m^*} . The behavior of peak II is consistent with the behavior predicted by Hoffman and Weeks, and it is therefore suggested that this peak results from the melting of relatively high-molecular-weight chain-folded lamellae.

In reported studies on multiple-melting behavior of polymers, various theories have been proposed to account for the phenomenon. These include melting and recrystallization,²³⁻²⁶ the existence of two or more distinct morphological forms,^{30,36} and the effects of orientation.³⁷ A factor that has largely been overlooked, however, is the role of molecular weight and molecular weight distribution during the crystallization process. Thus Harland et al.³¹ have shown, in respect to polyethylene, that samples of different molecular weight and molecular weight distribution may produce either single- or multiple-melting endotherms when crystallized or annealed. Similarly, Mandelkern et al.^{38,39} have shown that the rates of crystallization and melting temperatures observed for polyethylene are molecular weight dependent. Both sets of workers have shown that at moderate degrees of supercooling, preferential crystallization of high-molecular-weight material occurs. In addition, Harland et al. have shown that at low crystallization temperatures, the extent of crystallization increases with decreasing molecular weight and that the efficiency of fractionation is greater the higher the crystallizing or annealing temperature.

Although molecular weight fractionation has only been reported for polyethylene, it seems reasonable to assume that such a process must also occur in other polymers. It is suggested that peak I results from the melting of crystals of low-molecular-weight polymer that were formed by a fractionation process during crystallization. As shown in Figure 2, the peak temperature values of peak I cannot be used to obtain a value of T_{m^*} according to the theory of Hoffman and Weeks,⁷ since these values describe a line parallel to the line $T_{m,obs} = T_c$. It is suggested that this results because the theory of Hoffman and Weeks is only applicable to high-molecular-weight material.

From Figures 6 and 7 it appears that peak IV has a direct relationship with peak II. Thus at low crystallization temperatures, peak IV is present, but it begins to decrease in size and finally disappears as peak II develops. It is suggested that peak IV results from the melting of the same high-molecular-weight chain-folded lamellae as peak II. However, at low crystallization temperatures much thinner lamellae are formed, as a consequence of the low crystallization rate, and these are subject to partial melting and recrystallization in much the same manner as peak III crystals. As the crystallization temperature increases, the average lamellar thickness increases and peak II appears on the DSC traces. However, within the distribution of lamellar thicknesses, there is still a proportion of relatively thin lamellae that will melt and recrystallize, resulting in peak IV. At relatively high crystallization temperatures, the average lamellar thickness continues to increase, and at some definite value of T_c , under the conditions employed, none of these will be subject to recrystallization, and therefore peak IV disappears. The partial melting and recrystallization of thin lamellae has been discussed by Hoffman and Weeks,⁷ and the presence and behavior of peak IV on the DSC traces is to be expected.

The above interpretation of the behavior of peaks I-IV allows the salient features of the multiple-melting phenomena, shown in Table VI and Figures 6 and 7, to be described in some detail.

In the range of crystallization temperatures studied, it is suggested that preferential crystallization of high-molecular-weight material occurs. Such a fractionation process will alter the molecular weight distribution of the molten amorphous phase, and further crystallization will necessarily be associated with material of lower molecular weight. These low-molecular-weight crystals may contain a high concentration of chain-end defects and therefore will melt at a lower temperature, resulting in peak I. Increasing the crystallization temperature will increase the size and perfection of the low-molecular-weight crystals and hence the peak temperature of peak I. However, these crystals will always melt at temperatures well below the equilibrium melting temperature, even under favorable crystallization conditions.

At low crystallization temperatures the majority of crystallites formed from the high-molecular-weight material are relatively small and imperfect. However, a proportion of relatively perfect, though thin, chain-folded lamellae will also be formed. Both types of crystal melt and recrystallize during the heating cycle of the experiment. The driving force for recrystallization of the former, which gave rise to peak III, will be an increase in both their size and perfection, whereas that of the latter, which yields peak IV, will be an increase in lamellar thickness. The rate of melting of peak III type crystallites will be determined by the rate of heating,^{23,24} whereas the rate of recrystallization will be dependent on the degree of supercooling below the peak III melting temperature. At temperatures only slightly below the peak III melting temperature, there will be insufficient supercooling to allow further recrystallization, and at such temperatures the rate of melting will approach and finally exceed the crystallization rate. A similar situation can be envisaged for the thin lamellae.

As the crystallization temperature is increased, the high-molecular-weight material will show an increased tendency to crystallize as relatively perfect chain-folded lamellae in consequence of the increased rate of crystallization. This results in a gradual increase in the size of peak II and a corresponding decrease in the size of peak III, until at temperatures where the crystallization is

rapid, peak III disappears (Fig. 7) between $T_c = 170$ – 180°C . Such a situation would be expected to show a marked dependence on the time of crystallization, and this behavior has been reported by Holdsworth and Turner-Jones²⁴ for 2GT.

At high crystallization temperatures, a rapid decrease in size of peak II can be expected from the theory of Hoffman and Weeks as a consequence of the rapidly decreasing crystallization rate. With reference to Fig. 7, this can be seen to occur. Between $T_c = 180$ – 187.5°C , peak II gradually decreases in size; and between $T_c = 190$ – 192.5°C , the peak becomes a fraction of its original size.

Comparison of the traces obtained after crystallization at 190 and 192.5°C suggests that peak I has markedly increased in size. That this is not the case was shown by control experiments in which the cooling stage after crystallization was omitted and the sample was scanned from T_c . At these crystallization temperatures only one peak was observed in control experiments. This corresponded in size and peak temperature to peak II. The material responsible for the other endotherm must therefore have crystallized during cooling, giving rise to small and imperfect crystals of the peak III type. Thus peak I disappears and peak III reemerges. At $T_c = 192.5^\circ\text{C}$ the peak temperature of the "new" endotherm is only 1°C lower than the normal peak III temperature, whereas that at $T_c = 195^\circ\text{C}$ is almost identical to peak III. It is suggested that supporting evidence for this interpretation can be seen in Figure 8, which shows a DSC trace from a sample that had been cooled from the melt at $320^\circ\text{C}/\text{min}$ to 47°C and was

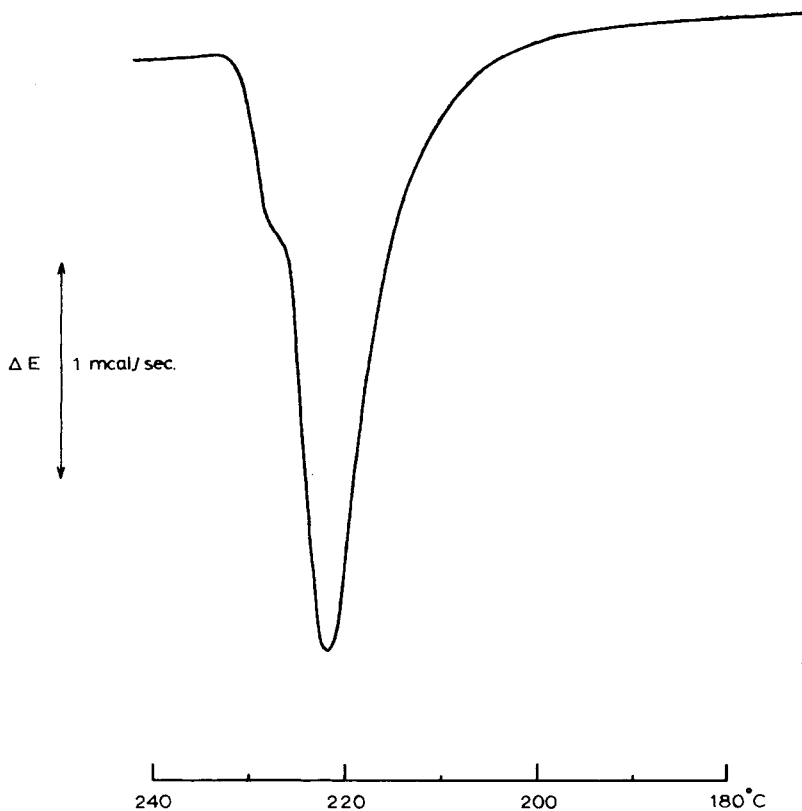


Fig. 8. Melting endotherms for a quenched, melt-pressed 4GT film.

then scanned at 20°C/min. This shows an endotherm that is almost identical in size, shape, and peak temperature to peak III. The reemergence of peak IV at $T_c = 195^\circ\text{C}$ results from crystallization during the cooling cycle.

The occurrence of more than one crystallization process—i.e., crystallization of relatively perfect chain-folded lamellae, crystallization of small and imperfect crystallites from high-molecular-weight material, and crystallization of low-molecular-weight material—may account for the fractional values of the Avrami exponent n shown in Table V. An increase in n from 2.0 to 2.5 was observed for 4GT between $\Delta T = 45\text{--}37.5^\circ\text{C}$. Gilbert and Hybart's results,⁵ which gave $n = 2.6/2.8$ for 4GT at $\Delta T \approx 24^\circ\text{C}$, suggest that an integral value of 3 is approached at very high crystallization temperatures, where the main equilibrium crystallization process occurs. According to Sharples,²² an n value of 3 corresponds to spherulic growth either from spontaneous or sporadic nuclei.

The double endotherms observed by Hobbs and Pratt³⁵ for nonisothermally crystallized samples of 4GT can be explained in terms of the interpretation of the peak behavior given in the present study. The latter authors showed that the low-temperature endotherm increased in size and the high-temperature endotherm decreased in size as the cooling rate decreased. Similarly, the peak temperature of the low-temperature endotherm increased, whereas that of the high-temperature endotherm remained constant with decreasing cooling rate. At high rates of cooling, small and imperfect crystals are formed, i.e., analogous to peak III crystals, and these melt and recrystallize during the heating cycle of the experiment, resulting in the high-temperature endotherm. The low-temperature endotherm is the result of the melting of relatively perfect chain-folded lamellae formed during cooling. As the cooling rate decreases, the lamellar thickness, and hence the size and peak temperature of this endotherm increases.

One of the authors (W.M.) thanks the Department of Polymer and Fibre Science for a Research Studentship.

References

1. W. Marrs, R. H. Peters, and R. H. Still, *J. Appl. Polym. Sci.*, **23**, 1063 (1979).
2. J. G. Smith, C. J. Kibler, and B. J. Sublett, *J. Polym. Sci.*, **4**, 1851 (1966).
3. G. Farrow, J. McIntosh, and I. M. Ward, *Markromol. Chem.*, **38**, 147 (1960).
4. A. Conix and R. Van Kerpel, *J. Polym. Sci.*, **40**, 521 (1959).
5. M. Gilbert and F. J. Hybart, *Polymer*, **13**, 327 (1972).
6. R. M. Shulken, R. E. Boy, and R. H. Cox, *J. Polym. Sci., Part C*, **6**, 17 (1964).
7. J. D. Hoffman and J. J. Weeks, *J. Res. Natl. Bur. Stand.*, **66A**, 13 (1962).
8. J. R. Knox, in *Analytical Calorimetry*, Vol. 1, R. S. Porter and J. F. Johnson, Eds., Plenum, New York, 1968, p. 45.
9. P. J. Flory, *Trans. Faraday Soc.*, **51**, 848 (1955).
10. C. H. Baker and L. Mandelkern, *Polym.*, **7**, 7 (1966).
11. M. H. Thiel and L. Mandelkern, *J. Polym. Sci., Part A*, **8**, 957 (1970).
12. I. Kirshenbaum, *J. Polym. Sci., Part A*, **3**, 1869 (1965).
13. P. J. Flory, L. Mandelkern, and H. K. Hall, *J. Am. Chem. Soc.*, **73**, 2532 (1951).
14. R. D. Evans, H. R. Mighton, and P. J. Flory, *J. Am. Chem. Soc.*, **72**, 2018 (1951).
15. R. C. Roberts, *Polymer*, **10**, 113 (1969).
16. K. Onder, R. H. Peters, and L. C. Spark, *Polymer*, **13**, 133 (1972).
17. L. Mandelkern, in *Crystallization of Polymers*, McGraw-Hill, New York, 1964, p. 90.
18. L. Mandelkern, in *Crystallization of Polymers*, McGraw-Hill, New York, 1964, Chap. 8.
19. J. B. Jackson and G. W. Longman, *Polymer*, **18**, 873 (1969).
20. F. J. Hybart and B. Pepper, *J. Appl. Polym. Sci.*, **13**, 2643 (1969).
21. S. Gogolewski and E. Turska, *J. Appl. Polym. Sci.*, **16**, 1959 (1972).

22. A. Sharples, *Introduction to Polymer Crystallization*, Arnold, London, 1966, Chap. 4.
23. R. C. Roberts, *J. Polym. Sci., Part B*, **8**, 381 (1970).
24. P. A. Holdsworth and A. Turner-Jones, *Polymer*, **12**, 195 (1971).
25. G. E. Sweet and J. P. Bell, *J. Polym. Sci., Part A*, **10**, 1273 (1972).
26. M. Ikeda, *Kobunshi Kagaku*, **25**, 87 (1968).
27. G. W. Miller, *Thermochim. Acta*, **8**, 129 (1974).
28. E. L. Lawton and D. M. Cates, *J. Appl. Polym. Sci.*, **13**, 899 (1969).
29. F. J. Hybart and J. D. Platt, *J. Appl. Polym. Sci.*, **11**, 1449 (1967).
30. J. P. Bell and J. H. Dumbleton, *J. Polym. Sci., Part A*, **7**, 1033 (1969).
31. W. G. Harland, M. M. Khadr, and R. H. Peters, *Polymer*, **13**, 13 (1972).
32. B. H. Clampitt, *Anal. Chem.*, **35**, 577 (1963).
33. Z. Pelzbauer and R. Manley, *J. Polym. Sci., Part A*, **8**, 649 (1970).
34. M. Jaffe and B. Wunderlich, *Kolloid. Z. Z. Polym.* **216/217**, 203 (1967).
35. S. Y. Hobbs and C. F. Pratt, *Polymer*, **16**, 462 (1975).
36. T. Kawai, K. Ehara, H. Sasano, and K. Kamide, *Makromol. Chem.*, **111**, 271 (1968).
37. T. R. White, *Nature*, **175**, 895 (1953).

Received August 25, 1977